Available online at www.sciencedirect.com
ScienceDirect
European Polymer Journal 43 (2007) 2891–2900
EUROPEAN POLYMER JOURNAL
www.elsevier.com/locate/europolj

Macromolecular Nanotechnology

Novel fluorescent amphiphilic block copolymers: Controllable morphologies and size by self-assembly

Xiaoju Lu, Shuling Gong, Lingzhi Meng *, Cheng Li, Feng Liang, Zhaoqiang Wu, Lifen Zhang

Department of Chemistry, Wuhan University, Wuhan 430072, PR China

Received 16 March 2006; received in revised form 28 March 2007; accepted 4 April 2007
Available online 19 April 2007

Abstract

New fluorescent amphiphilic copolymers polyacrylamide-*b*-poly(*p*-methacrylamido)acetophenone thiosemicarbazone (PAM-*b*-PMATC) were synthesized by atom transfer radical polymerization (ATRP) method. The structures of polymers were confirmed by ^{1}H NMR and gel permeation chromatography–multi-angle laser light scatting (GPC–MALLS). PAM-*b*-PMATC showed a broad emission peak about 388 nm excited at 318 nm in aqueous solution. The self-assembly behavior of PAM-*b*-PMATC in the binary mixture formamide/water was observed by transmission electron microscope (TEM). It indicated that PAM-*b*-PMATC-I and -II with the same PAM block self-assembled to vesicles and sunflower-like micelles. The water fraction in the mixture could control the size and thickness of vesicles. Vesicle size increased from 50 to 420 nm and vesicle thickness changed from 5 to 50 nm with water content ranging from 33 to 90 vol.%. In addition, the cytotoxicity in vitro of PAM-*b*-PMATC-I and its nanoparticles loaded with methotrexate (MTX) were evaluated by MTT assay.

Keywords: Amphiphilic copolymer; Fluorescent; Self-assembly; Vesicles

1. Introduction

The self-assembly of amphiphilic polymers has resulted in assembles such as spheres, rods, vesicles, large compound micelles, nanofibers and nanotubes [1–7]. The morphology of the aggregates is a function of several variables, such as compositions and blocks length of copolymers, concentration and chain architectures of copolymers, solvents, additives and so on [8–11]. Among the different morphologies which have obtained thus far for amphiphilic polymers, vesicles are possibly the most interesting morphology from the point of view of potential applications in such fields as microreactor chemistry, pharmacology, medicine and cosmetics [12]. In this context, the control of the micellar morphology is of great importance to obtain the desired functions and properties.

Fluorescence techniques are used as versatile tools to monitor the solution properties with exquisite sensitivity and selectivity which can determine the aggregation number of the hydrophobic core and the critical aggregation concentration [13,14]. Fluorescent labeling polymeric vesicles can be

* Corresponding author. Tel.: +86 27 87219094; fax: +86 27 68754067.
E-mail address: lzhmeng@whu.edu.cn (L. Meng).

0014-3057/$ - see front matter
doi:10.1016/j.eurpolymj.2007.04.006

achieved through following approaches: encapsulate a water-soluble fluorescent dye during vesicle formation, and link a certain percentage of fluorophore to membrane molecules and aggregate a lipophilic probe in the hydrophobic part of the membrane [15,16]. Generally amphiphilic polymers with intrinsic fluorescence are labeled with naphthalene or pyrene. Short poly(ethylene oxide) chains labeled at one end with pyrene in water were found to form micelles [17]. In contrast, the research on morphology of amphiphilic polymers with intrinsic fluorescence has not been studied in detail.

Atom transfer radical polymerization (ATRP) is an extremely active area of polymer synthesis research [18]. Amphiphilic copolymers based on polyacrylamide derivatives polymerized by ATRP are of increasing interest because of their specific solution properties, such as micellization, thermosensitivity, and pH sensitivity [19,20]. In this contribution, functional monomer (*p*-methacrylamido)acetophenone thiosemicarbazone (MATC) was synthesized and amphiphilic polyacrylamide-*b*-poly(*p*-methacrylamido)acetophenone thiosemicarbazone (PAM-*b*-PMATC) copolymers was prepared by ATRP. Hydrophobic MATC functional moiety has both intrinsic fluorescent and pharmacological versatilities such as antibacterial, antitumoral, antiviral, and anticonvulsant [21,22].

The first observation of block copolymer vesicles with small hydrophilic fractions (<20%) was reported by Eisenberg and co-workers [8]. There have been reports on block polymer vesicle with a hydrophilic fraction $35 \pm 10\%$ [23] and hydrophilic fraction (>60%) [24]. Herein we reported the preparation of a new kind of polymer vesicle with a controlled size from well-defined copolymers having a higher hydrophilic fraction (80%). This provides an efficient way to obtain intrinsic fluorescent polymeric vesicles with high hydrophilic fraction. To our knowledge, copolymer vesicles with such a high hydrophilic fraction have not yet been investigated.

Water-soluble fluorescent polymer can be used as a promising fluorescent probe for measurements of biomacromolecules and cells [25]. Carbohydrate-functioned fluorescent polymers can been used to detect bacteria [26]. Herein, we show that these fluorescent polymer vesicles could be potentially used as drug carriers and fluorescent tracer to determine the drug release behavior in drug delivery by fluorescent technology.

2. Experimental part

2.1. Materials

Acrylamide (AM) was recrystallized from acetone twice (Tianjing Chemical Reagents Co., China), Bipyridine (bpy) was recrystallized from acetone (Shanghai Chemical Reagents Co., China), CuBr (Aldrich, 98%) was purified by stirring in acetic acid, washing with methanol, and then drying in vacuum. $CuBr_2$ and glycerol were used as received. Aminothiourea (Shanghai Chemical Reagents Co., 99%), *p*-aminoacetophenone (Acros Organics, 99%), methotrexate (MTX), *N*,*N*-dimethylformamide (DMF) and α-bromopropionamide (α-Br-PA) were used as received. All the other chemicals used were purified according to conventional methods or used received.

2.2. Synthesis of (*p*-methacrylamido)acetophenone thiosemicarbazone (MATC) monomer

The monomer (*p*-methacrylamido)acetophenone thiosemicarbazone was synthesized according to the method described by Li et al. [27]. 3.37 g (37 mmol) aminothiourea was dissolved in 120 ml of deionized water and 1.5 ml of acetic acid at 75 °C, under stirring 75 ml ethanol solution of *p*-aminoacetophenone (5.0 g; 37 mmol) was added dropwise into the system and the mixture was maintained at 85 °C for 15 h. Most of ethanol was removed under reduced pressure, and the slight yellow solid *p*-aminoacetophenone thiosemicarbazone was obtained by precipitated in distilled water and dried at 45 °C under vacuum. 2.08 g (10 mmol) of *p*-aminoacetophenone thiosemicarbazone was dissolved in mixture solution of 50 ml of acetone and 0.89 ml (11 mmol) of pyridine. Under ice–salt bath, 15 ml of acetone solution of 1.06 ml (11 mmol) methacryloyl chloride was added dropwise, and the solution was stirred at room temperature for 5 h. Then a large amount of water was poured into the solution under stirring to precipitate the product. The collected product was reprecipitated three times from acetone and placed under vacuum to give slight yellow powder (*p*-methacrylamido)acetophenone thiosemicarbazone, melting range: 201–204 °C. IR (KBr, cm^{-1}): 3420, 3310, 3272, 3514, 1658, 1622, 1593, 1533, 1489, 1449, 1407, 1285, 1247, 1088, 947, 840, 542. ^1H NMR (300 MHz, $CDCl_3$): δ (ppm): 1.98 (s, 3H, $CH_2{=}CCH_3$), 2.18 (s, 3H, $N{=}CCH_3$), 5.41 and 5.72 (each s, $1H \times 2$,

C=CH_2), 6.25 and 7.24 (each s 1H × 2, S=CNH_2), 7.50–7.62 (AA′BB′, 2H × 2, Ar*H*), 7.52 (s, 1H, PhN*H*), 8.63 (s, 1H, S=CN*H*). Elemental analysis: Calcd. for $C_{13}H_{16}N_4OS$: C, 56.50; H, 5.80; N, 20.27; S, 11.60. Found: C, 56.24; H, 5.87; N, 20.20; S, 11.38. Electrospray ionization-mass spectrometer (ESI-MS): *m*/*z* (RI): 277 (MH^+, 45).

2.3. Synthesis of polyacrylamide-Br (PAM-Br) macroinitiator

Polymerization was conducted in a predried three-neck round-bottom flask with a magnetic stir bar. In a typical polymerization using glycerol:water mixture 1:2 (v/v), AM and solvent were purged with nitrogen for 15 min, then CuBr, bpy and α-Br-PA ([AM]:[CuBr]:[bpy]:[α-Br-PA] = 200:1:2:1 (molar ratio)) were quickly added to the flask under nitrogen. After closing the flask with rubber septum, it was evacuated and back-filled with nitrogen three times, then the flask was placed in a preheated oil bath maintained at 120 °C. After 24 h, the polymer was precipitated into three-fold methanol. The precipitated polymer was separated by centrifugation, redissolved in a minimum amount of water, and reprecipitated into methanol. This procedure was repeated for three times. The polymer was dried in a vacuum oven at 50 °C for 48 h.

2.4. Synthesis of polyacrylamide-b-poly-(p-methacrylamido)acetophenone thiosemicarbazone (PAM-b-PMATC) block copolymer by ATRP

PAM-*b*-PMATC diblock copolymer was synthesized by ATRP in formamide. In a typical run, 25 ml round-bottom flask was charged with macroinitiator PAM-Br and catalyst CuBr/bpy ([PAM-Br]:[CuBr]:[bpy] = 1:1:2 (molar ratio)) and formamide under nitrogen for 15 min, then different amount of monomer MATC was quickly added to the mixture. After closing the flask with rubber septum, the system was evacuated and back-filled with nitrogen three times. The flask was placed in a preheated oil bath and maintained at 100 °C under stirring for 24 h. The following experimental procedure was similar to the above.

2.5. Preparation of micelles in aqueous solution

To prepare the aggregates in aqueous solution, the PAM-*b*-PMATC copolymers were dissolved in formamide/water mixture with varying water content (33, 50, 75 and 90 wt.%) by stirring for 48 h, and the initial copolymer concentration in formamide/water mixture was 5 wt.%. Then, a large amount of water was added to the resulting solutions to quench the aggregate morphologies. Subsequently, the resulting solution was placed in dialysis bags and dialyzed against distilled water for 72 h to remove all of the organic solvent from the solution, and a final concentration of solution was 2 g/l.

2.6. Preparation of polymeric nanoparticles loaded with methotrexate (MTX)

The polymeric nanoparticles were prepared by the dialysis technique. 10 mg copolymer and 1 mg model drug methotrexate were dissolved in 4 ml mixture of formamide/DMF (3/1 v/v). The solution was stirred at room temperature for 1 h, and 10 ml distilled water was added slowly and kept stirring for 1 h, then the resulting solution was placed in dialysis bags and dialyzed against distilled water for 24 h to remove all of the organic solvent from the solution. The suspension was passed through 0.45 mm filter to remove aggregates. To determine the drug loading content and entrapment efficiency, polymeric nanoparticles were dissolved in formamide/DMF (3/1, v/v) and then measured with ultraviolet–visible (UV–vis) spectrophotometer at 303 nm.

2.7. Instruments

All ^{1}H NMR spectra were recorded on a Varian Mercury VX-300 MHz spectrometer (USA). Elemental analysis was conducted on a Flash EA 1112 series elemental autoanalyzer (Italy). Mass spectrum was obtained on an LCQ-Advantage electrospray ionization-mass spectrometer (ESI-MS) (Finnigan, England). Steady-state fluorescence spectra in different concentration of copolymer solution were obtained on a Shimadzu RF-5301PC spectrometer (Japan) at room temperature. Ultraviolet–visible (UV–vis) spectra were taken on a TU-1901 spectrometer (China).

Gel permeation chromatography–multi-angle laser light scatting (GPC–MALLS) was convenient for determination of the true molecular weight and molecular weight distribution of polymer without standard sample. Number molecular weights M_n, and polydispersity M_w/M_n of the samples were determined by a DAWN®DSP multi-angle laser photometer in formamide at a flow rate of 1.00 ml/min at 25 °C.

2.8. Transmission electron microscope (TEM) observation

The size and morphology of copolymer aggregates were recorded by a JEM-100CXII transmission electron microscope (Japan). The dialyzed polymer solutions were placed onto the TEM copper grid covered by a polymer support film. After 15 min, the excess solution was allowed to dry in atmosphere and at room temperature for 2 h before observation.

2.9. In vitro cytotoxicity test

The cytotoxicity of PAM-*b*-PMATC-I and its nanoparticles loaded with methotrexate (MTX) were evaluated by using the MTT assay according to the method of Mosmann [28]. Five thousand A549 cells/well, MTT solution 2.0 g/l and Hank's balanced salt solution (HBSS) as a medium were selected to carry out the cytotoxicity tests. The test was performed as follows: after A549 cells were attached to the 96 wells and incubated for 24 h at 37 °C, the different concentration of PAM-*b*-PMATC-I and its nanoparticles dissolved in HBSS were added to the wells. To each well 50 μl of MTT solution was added after the wells were incubated for another 72 h at 37 °C. The plates were incubated for an additional 4 h at 37 °C and the MTT solution was removed. Negative (HBSS) control wells were treated similarly as above. Absorbance was measured spectrophotometrically at 550 nm using a MuLTiskAn MK3 unit. Cell viability (as a percent of the negative control) was calculated from the absorbance values.

3. Results and discussion

3.1. Synthesis of fluorescent amphiphilic polymers PAM-b-PMATC

Atom transfer radical polymerization (ATRP) has been demonstrated to produce polymers with well-controlled architecture, predictable molecular weight and narrow polydispersity [18]. Moreover, the chemistry of ATRP is tolerant of many functional groups, thereby permitting the controlled synthesis of a broad range of polymers with novel structures and topologies. Novel fluorescent amphiphilic copolymers were synthesized by ATRP based on MATC as hydrophobic segment and PAM as hydrophilic segment. The synthesis route was given in Fig. 1.

More recently, Mandal's group has thoroughly investigated the ATRP of acrylamide in the mixture of water and glycerol [29,30]. According to literature [29], PAM-Br was obtained by ATRP in glycerol–water mixture (1:1, v/v). The conversion of PAM-Br was 60% by gravimetry, and M_n and the M_w/M_n was 1.5×10^4 g/mol and 1.74, respectively. In order to obtain copolymers with different hydrophobic segment, the ratio of monomer (MATC) to macroinitiator (PAM-Br) was varied. Using PAM-Br as macroinitior, two fluorescent copolymers were synthesized by ATRP in formamide. The ^{1}H NMR spectrum of PAM-*b*-PMATC-II was shown in Fig. 2. The proton signals appeared between 1.3 and 2.3 ppm were assigned to the saturated protons of the CH_3, CH_2 and CH groups of main chains. The signal at about 3.4 ppm was assigned to terminated C(CH_3)—Br in PMATC unit. The resonances

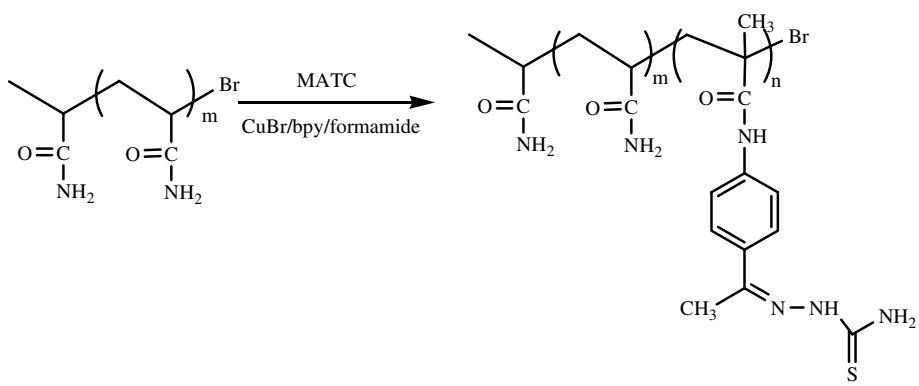

Fig. 1. Synthesis route of block copolymers PAM-*b*-PMATC by ATRP using macroinitiator.

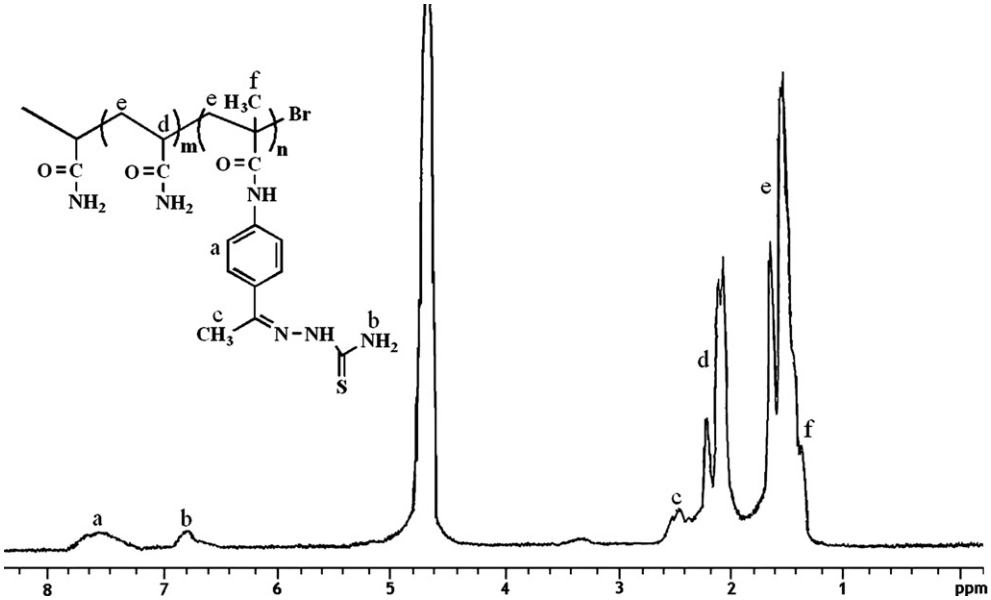

Fig. 2. ^{1}H NMR spectrum of PAM-*b*-PMATC-II in D_2O.

of protons for the phenyl groups of PMATC repeat unit occurred at the chemical shifts 7.0–7.6 ppm.

Copolymer composition was determined by ^{1}H NMR spectroscopy [31,32]. The hydrophobic content was calculated from the relative integrated area of peak a corresponding to the protons of the phenyl groups of the hydrophobic chains compared to that of peak d corresponding to the protons of CH groups in the hydrophilic backbone. The composition and molecular weight data of amphiphilic copolymer were summarized in Table 1.

3.2. Critical micelle concentration (CMC) in aqueous solution

The critical micelle concentration (CMC) value of copolymer solution can be determined by fluorescence measurements from its intrinsic fluorescence. It is known that the fluorescent behavior of the intrinsic probe can reflect the dynamics of the polymer backbone in the solution [27,33]. As indicated in Fig. 3, the copolymers showed specific emission maximum at 388 nm excited at 318 nm. The emission band centered at 388 nm was attributed to the direct excitation of phenyl groups. Inset gave out the fluorescence intensity versus concentration of PAM-*b*-PMATC-I in aqueous solution. The fluorescent intensity increased, reached a maximum intensity and then decreased gradually with increasing copolymer concentration. This maximum intensity at the concentration of 1.5×10^{-2} g/l could be the CMC for PAM-*b*-PMATC-I. The CMC of PAM-*b*-PMATC-II was about 2×10^{-1} g/l, which was higher than that of PAM-*b*-PMATC-I. The value of CMC increased with decreasing the hydrophobic content of copolymer with the same length of hydrophilic chain. Above CMC, the amphiphilic polymer coils

Table 1
GPC and ^{1}H NMR data of PAM-*b*-PMATC

Entry	Conversion (%)	GPC–MALLS[a]		^{1}H NMR[b]		
		M_n (g/mol)	M_w/M_n	M_n (g/mol)	wt.% PAM	wt.% PMATC
PAM-Br	60	1.5×10^4	1.74			
PAM-*b*-PMATC-I	63	2.3×10^4	1.95	1.87×10^4	80	20
PAM-*b*-PMATC-II	55	2.1×10^4	1.88	1.58×10^4	95	5

[a] M_n and M_w/M_n estimated from GPC–MALLS.
[b] Number molecular weight of the block copolymer calculated from ^{1}H NMR and M_n of the first block PAM-Br.

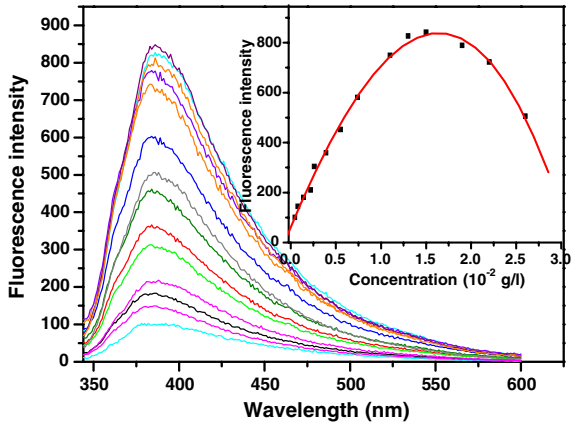

Fig. 3. Fluorescent emission spectra at different concentration of PAM-*b*-PMATC-I (5×10^{-5} to 2.7×10^{-2} g/l) excited at 318 nm. Inset: fluorescence intensity at 388 nm versus concentration.

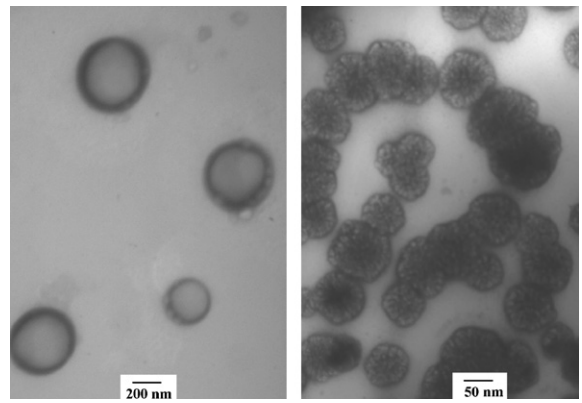

Fig. 4. TEM images of aggregates from PAM-*b*-PMATC-I (left) and PAM-*b*-PMATC-II (right) at a concentration of 2 g/l in binary mixture formamide/water (10/90, v/v).

associate to form large aggregates, thus the concentration of fluorophore will be high enough in the interchain hydrophobic domains to cause fluorescence self-quenching [34,35]. While below the CMC, fluorescence intensity increases nearly linearly as the concentration increasing.

The CMC values are most commonly employed to evaluate the thermodynamic stability of the polymeric micelles in aqueous solutions [36]. Amphiphilic polymers generally have remarked lower CMC values (usually at 10^{-6} M) [37,38]. In our case, the CMC value of PAM-*b*-PMATC-I is 1.5×10^{-2} g/l, about 10^{-6} M. The lower CMC value illustrates the effectiveness of structure for stabilizing vesicle-like aggregates.

3.3. Morphologies of PAM-b-PMATC aggregation

Commercial applications of those different nanostructures call for a high degree of control on the morphology of the resulting materials. Eisenberg and his co-workers [8] described the morphology of polystyrene-*b*-poly(acrylic acid) (PS-*b*-PAA) copolymer changed from vesicles to rods then to spheres with a decrease in the block length ratio of hydrophobic segments PS to hydrophilic segments PAA in DMF/water solution. Namely the lower the block length ratio was of PAA to PS, the greater the tendency was to form vesicles.

The aggregative behavior of PAM-*b*-PMATC aqueous solutions at concentration of 2 g/l was examined by TEM. Typical TEM images of PAM-*b*-PMATC aggregative morphology were shown in Fig. 4. A morphology transition from vesicles to sunflower-like micelles was observed as a decrease in the block length ratio of PMATC to PAM in binary formamide/water mixture. To our understanding, under this condition, hydrophobic PMATC blocks tend to form the core of a micelle, whereas hydrophilic PAM chains form the corona. In the hydrophilic region, the corona repulsion increases with increasing PAM block length. At given water content in the system, with similar PAM block length in PAM-*b*-PMATC-I and -II, the decrease in molar ratio of PMATC to PAM induces PAM-*b*-PMATC-I and -II different aggregation morphology. This suggests that the molar ratio of hydrophobic segments to hydrophilic segments plays an important role in triggering the micelle morphology of block copolymer.

3.4. The effect of water content on the size and thickness of PAM-b-PMATC vesicles

To further explore the dynamics of vesicles and more direct visualization of the size and thickness of copolymer vesicles, water content in formamide/water solvent mixture was varied for PAM-*b*-PMATC-I. TEM morphologies showed that the size and thickness of vesicles increased with water content increased. Fig. 5 illustrated vesicles size changed of PAM-*b*-PMATC-I resulting from water content. The study revealed that when water content at 33 vol.% (Fig. 5a), vesicles with diameter from 30 to 80 nm and wall thickness about 5 nm were observed. When water content up to 50 vol.%

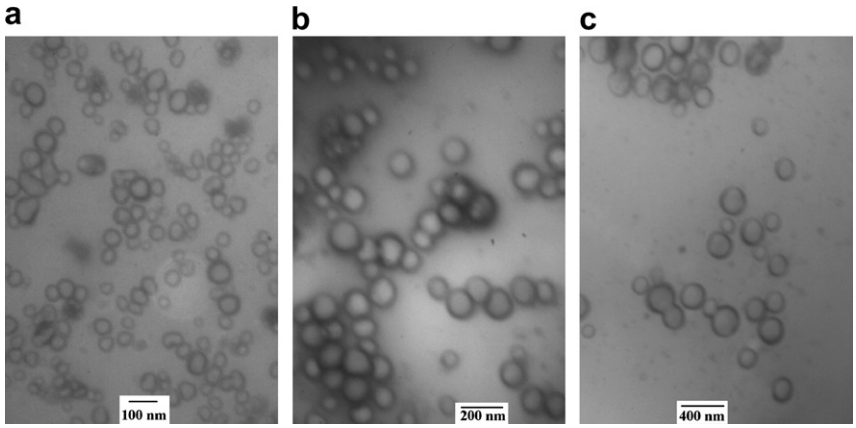

Fig. 5. TEM images of vesicles of PAM-*b*-PMATC-I copolymer with concentration at 2 g/l in the binary solvent mixture of formamide and water, water fractions (v/v): (a) 33; (b) 50; (c) 75.

(Fig. 5b), the vesicle increased in diameter from 70 to 120 nm and wall thickness increased to 8 nm, and vesicles contacted and adhered. An increase of water content to 75 vol.% (Fig. 5c), vesicles diameter grew from 100 to 200 nm and wall thickness became about 15 nm, and contact and fusion between two vesicles were observed. Vesicles showed a mean diameter from 200 to 420 nm and the wall thickness increased from 15 to 40 nm as the water content increased to 90 vol.%, and vesicles separated completely, with some vesicles forming a uniform outer wall and others fusing immaturely (Fig. 4 left).

Eisenberg et al. had suggested that the size of the PS-*b*-PAA copolymer vesicles was under thermodynamic control [39]. As demonstrated as above for PAM-*b*-PMATC-I, water content in mixture of formamide/water plays a key role in tuning the size and thickness of vesicles. To be able to accommodate water within the inner core of the vesicles, some hydrophilic segments need to be oriented toward the cavity of the vesicle. Hence, at low water content, the medium is not a good solvent for the PAM segments, the macromolecule is not expanded in the medium and so the vesicles are small. With increasing water content, the solvent becomes worse for the core block but better for corona block; therefore, the system attempts to decrease the total interfacial area, and vesicles fusion occurs, resulting in an increase in the vesicle size and a decrease in the total number of particles. Water content ranged from 33 to 90 vol.%, and vesicle size increased from 50 to 420 nm and thickness grew from 5 to 50 nm.

3.5. The drug-loaded efficiency of PAM-b-PMATC-I

In order to investigate the ability of drug-loaded with PAM-*b*-PMATC-I, methotrexate (MTX), an anti-cancer drug, was used as a model drug. MTX could be easily encapsulated in the hydrophobic core of PAM-*b*-PMATC-I due to hydrophobic interaction [40]. Morphology of nanoparticles was observed by TEM and the image was presented in Fig. 6. The study showed that nanoparticles were regularly spherical in shape with diameter from 150 to 350 nm. The drug loading content and entrapment efficiency of PAM-*b*-PMATC-I were measured by UV spectrometer. The drug loading content was 5.5% and entrapment efficiency was 26%. That is, methotrexate is successfully loaded into the hydrophobic core of amphiphilic copolymer PAM-*b*-PMATC-I.

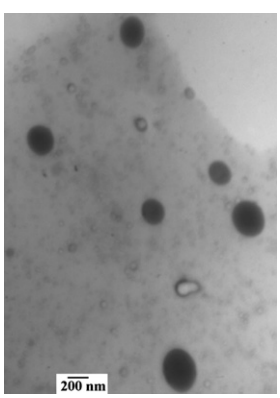

Fig. 6. TEM images of MTX-loaded PAM-*b*-PMATC-I with concentration at 0.5 g/l in aqueous solution.

3.6. Cytotoxicity of PAM-b-PMATC-I and nanoparticles in vitro

In order to evaluate the cytotoxicity of copolymer PAM-*b*-PMATC-I and MTX-loaded nanoparticles in vitro, A549 cells were used and MTT assays were carried out. MTT tests showed that both of them could inhibit A549 cells growth as the concentration increasing from 1×10^{-4} to 1×10^{-1} g/l. Fig. 7 gave the photomicrographs of the A549 cells cultured in the well for 72 h added with PAM-*b*-PMATC-I polymer solution and MTX-loaded nanoparticles solution, respectively. As shown in Fig. 7, there were much more cells in Fig. 7b than that in Fig. 7c. The results indicate that nanoparticles have better inhibition effect on A549 cells grow than polymer solution at the same concentration. The slight inhibition effect of block polymer on A549 cells may due to hydrophobic MATC functional moiety owning pharmacological versatilities [21,22]. The good inhibition effect of nanoparticles on A549 cells is ascribed to that nanoparticles release MTX drug slowly.

In Fig. 8, as the concentration increased from 1×10^{-4} to 1×10^{-1} g/l, PAM-*b*-PMATC-I had an ability to inhibit A549 cells growth, and the inhibition ratio decreased distinctly with the decrease of polymer concentration; but nanoparticles loaded with MTX had a stable inhibition ability, and the inhibition ratio remained above 40%. The inhibition ability of nanoparticles loaded with MTX changed slowly with concentration. The stable inhibition ability means nanoparticles release the encapsulated drug slowly and inhibit A549 cells growth stably.

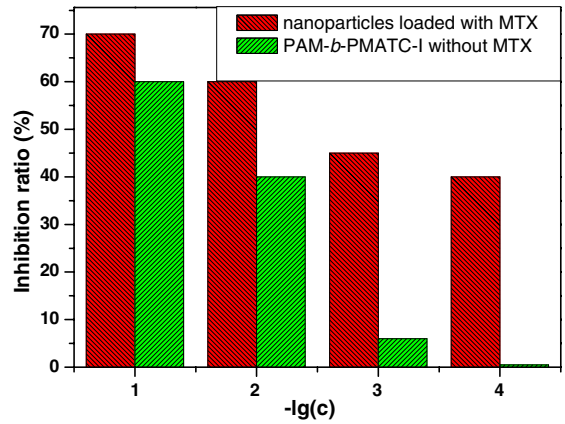

Fig. 8. Inhibition ratio versus solution concentration of PAM-*b*-PMATC-I and its nanoparticles, c: (g/l).

We assume that block polymer micelles load the hydrophobic drug inside the micelle core. When they release hydrophobic drug from the core, they achieve sustained release. The fluorescent amphiphilic copolymer can be developed to efficient drug delivery systems.

4. Conclusion

Fluorescent amphiphilic copolymers bearing PAM and PMATC were obtained by ATRP. The copolymer showed a specific fluorescence emission maximum at 388 nm excited at 318 nm in aqueous solution. TEM studies indicated PAM-*b*-PMATC self-assembled vesicles, sunflower-like micelles in binary mixture formamide/water. The lower the block length ratio was of PAM to PMATC, the greater the tendency was to form vesicles. The size

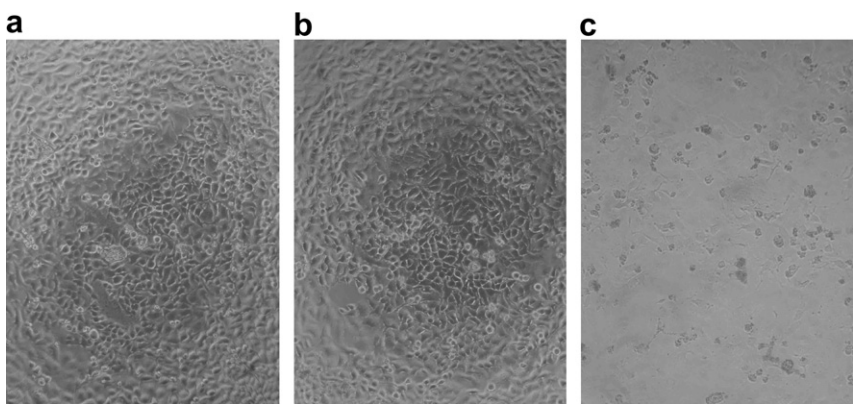

Fig. 7. Photomicrographs of the A549 cells cultured for 72 h in the well: (a) A549 cells; (b) A549 cells adding 1×10^{-3} g/l PAM-*b*-PMATC-I solution; (c) A549 cells adding 1×10^{-3} g/l nanoparticles loaded with MTX.

and thickness of vesicles increased with water content increase. In addition, the block polymer could load the hydrophobic anti-cancer drug inside the micelle core and maintain sustained drug release in vitro.

Acknowledgements

The authors are grateful to National Natural Science Foundation for financial support (Grant No. 20474044), and Prof. Xiao-Juan Xu, Ms. Yong-Zhen Tao, Ms. Li Li and Ms. Xi Yang, Department of Chemistry, Wuhan University, for their help in GPC–MALLS, TEM observation and fluorescence spectra determination, respectively.

References

[1] Liu G, Ding J, Guo A, Herfort M, Bazett-Jones D. Potential skin layers for membranes with tunable nanochannels. Macromolecules 1997;30(6):1851–3.
[2] Yan X, Liu F, Li Z, Liu G. Poly(acrylic acid)-lined nanotubes of poly(butyl methacrylate)-*block*-poly(2-cinnamoyloxyethyl methacrylate). Macromolecules 2001;34(26):9112–6.
[3] Jenekhe SA, Chen XL. Self-assembly of ordered microporous materials from rod-coil block copolymers. Science 1999;283(5400):372–5.
[4] Liu G, Qiao L, Guo A. Diblock copolymer nanofibers. Macromolecules 1996;29(16):5508–10.
[5] Zhang L, Eisenberg A. Morphogenic effect of added ions on crew-cut aggregates of polystyrene-*b*-poly(acrylic acid) block copolymers in solutions. Macromolecules 1996;29(27):8805–15.
[6] Borisov OV, Zhulina EB. Morphology of micelles formed by diblock copolymer with a polyelectrolyte block. Macromolecules 2003;36(26):10029–36.
[7] Zhou Z, Li Z, Ren Y, Hillmyer MA, Lodge TP. Micellar shape change and internal segregation induced by chemical modification of a tryptych block copolymer surfactant. J Am Chem Soc 2003;125(34):10182–3.
[8] Zhang L, Eisenberg A. Multiple morphologies of "crew-cut" aggregates of polystyrene-*b*-poly(acrylic acid) block copolymers. Science 1995;268(5218):1728–31.
[9] Yu Y, Eisenberg A. Control of morphology through polymer–solvent interactions in crew-cut aggregates of amphiphilic block copolymers. J Am Chem Soc 1997;119(35):8383–4.
[10] Van der Maarel JRC, Groenewegen W, Egelhaaf SU, Lapp A. Salt-induced contraction of polyelectrolyte diblock copolymer micelles. Langmuir 2000;16(19):7510–9.
[11] Ding J, Liu G. Growth and morphology change of polystyrene-*block*-poly(2-cinnamoylethyl methacrylate) particles in solvent–nonsolvent mixtures before precipitation. Macromolecules 1999;32(25):8413–20.
[12] Luo L, Eisenberg A. Thermodynamic stabilization mechanism of block copolymer vesicles. J Am Chem Soc 2001;123(5):1012–3.
[13] Yekta A, Xu B, Duhamel J, Adiwidjaja H, Winnik MA. Fluorescence studies of associating polymers in water: determination of the chain end aggregation number and a model for the association process. Macromolecules 1995;28(4):956–66.
[14] Beaudoin E, Hiorns RC, Borisov O, Francois J. Association of hydrophobically end-capped poly(ethylene oxide). 1. Preparation of polymers and characterization of critical association concentrations. Langmuir 2003;19(6):2058–66.
[15] Koyama Y, Umehara M, Mizuno A, Itaba M, Yasukouchi T, Natsume K. Synthesis of novel poly(ethylene glycol) derivatives having pendant amino groups and aggregating behavior of its mixture with fatty acid in water. Bioconjugate Chem 1996;7(3):298–301.
[16] Kita-Tokarczyk K, Grumelard J, Haefele T, Meier W. Block copolymer vesicles-using concepts from polymer chemistry to mimic biomembranes. Polymer 2005;46(11):3540–63.
[17] Laukkanen A, Winnik FM, Tenhu H. Pyrene-labeled graft copolymers of *N*-vinylcaprolactam: synthesis and solution properties in water. Macromolecules 2005;38(6):2439–48.
[18] Matyjaszewski K, Xia J. Atom transfer radical polymerization. Chem Rev 2001;101(9):2921–90.
[19] Ding S, Radosz M, Shen Y. Atom transfer radical polymerization of *N*,*N*-dimethylacrylamide. Macromol Rapid Commun 2004;25(5):632–6.
[20] Masci G, Giacomelli L, Crescenzi V. Atom transfer radical polymerization of *N*-isopropylacrylamide. Macromol Rapid Commun 2004;25(4):559–64.
[21] Beraldo H, Gambinob D. The wide pharmacological versatility of semicarbazones, thiosemicarbazones and their metal complexes. Mini-Rev Med Chem 2004;4(1):31–9.
[22] Chough YS. Synthesis and biological actions of derivatives of ethylenediamine, thiosemicarbazone, thiourea, hexachlorophene, acid amides, and Mannich bases. Yakhak Hoechi 1974;18(1):1–10.
[23] Discher BM, Won YY, Ege DS, Lee JC-M, Bates FS, Discher DE, et al. Tough vesicles made from diblock copolymers. Science 1999;284(5417):1143–6.
[24] Zhou Y, Yan D. Supramolecular self-assembly of giant polymer vesicles with controlled sizes. Angew Chem Int Ed 2004;43(37):4896–9.
[25] Wu Z, Gong S, Li C, Zhang Z, Huang W, Meng L. Novel water-soluble fluorescent polymer containing recognition units: synthesis and interactions with PC12 cell. Eur Polym J 2005;41(9):1985–92.
[26] Disney MD, Zheng J, Swager TM, Seeberger PH. Detection of bacteria with carbohydrate-functionalized fluorescent polymers. J Am Chem Soc 2004;126(41):13343–6.
[27] Li C, Meng L, Lu X, Wu Z. Thermo- and pH-sensitivities of thiosemicarbazone-incorporated fluorescent amphiphilic poly(*N*-isopropylacrylamide). Macromol Chem Phys 2005;206(18):1870–7.
[28] Mosmann T. Rapid colorimetric assay for cellular growth and cytotoxic assays. J Immunol Methods 1983;65(1–2):55–63.
[29] Jewrajka SK, Mandal BM. Living radical polymerization. 1. The case of atom transfer radical polymerization of acrylamide in aqueous-based medium. Macromolecules 2003;36(2):311–7.
[30] Jewrajka SK, Mandal BM. Living radical polymerization. II. Improved atom transfer radical polymerization of acrylamide in aqueous glycerol media with a novel

pentamethyldiethylenetriamine-based soluble copper(I) complex catalyst system. J Polym Sci: Polym Chem 2004; 42(10):2483–94.
[31] Volpert E, Selb J, Candau F. Influence of the hydrophobe structure on composition, microstructure, and rheology in associating polyacrylamides prepared by micellar copolymerization. Macromolecules 1996;29(5):1452–63.
[32] Xue W, Hamley IW, Castelletto V, Olmsted PD. Synthesis and characterization of hydrophobically modified polyacrylamides and some observations on rheological properties. Eur Polym J 2004;40(1):47–56.
[33] Winnik FM. Photophysics of preassociated pyrenes in aqueous polymer solutions and in other organized media. Chem Rev 1993;93(2):587–614.
[34] Wu SK, Li FM. New trends in photochemistry of polymers. Amsterdam: Elsevier; 1985. 85.
[35] Rutkaite R, Buika G, Grazulevicius JV. Fluorescence properties of carbazolyl-containing amphiphilic copolymers. J Photochem Photobiol A: Chem 2001;138(3):245–51.
[36] Kataoka K, Harada A, Nagasaki Y. Block copolymer micelles for drug delivery: design, characterization and biological significance. Adv Drug Deliv Rev 2001;47(1): 113–131.
[37] Kabanov AV, Batrakova EV, Alakhov VY. Pluronic block copolymers as novel polymer therapeutics for drug and gene delivery. J Control Release 2002;82(2–3):189–212.
[38] Xu J, Ji J, Chen W, Shen J. Novel biomimetic surfactant: synthesis and micellar characteristics. Macromol Biosci 2005;5(2):164–71.
[39] Luo L, Eisenberg A. Thermodynamic size control of block copolymer vesicles in solution. Langmuir 2001;17(22): 6804–6811.
[40] Zhang Y, Zhuo R. Synthesis and drug release behavior of poly(trimethylene carbonate)–poly(ethylene glycol)–poly(trimethylene carbonate) nanoparticles. Biomaterials 2005; 26(14):2089–94.